Acta Oceanol. Sin., 2022, Vol. 41, No. 4, P. 68–79
https://doi.org/10.1007/s13131-021-1829-8
http://www.aosocean.com
E-mail: ocean2@hyxb.org.cn

Contraction and warming of Antarctic Bottom Water in the Amundsen Sea

Yu Bai[1], Liang Zhao[1]*, Jingen Xiao[2], Shiying Lin[1]

[1] College of Marine and Environmental Sciences, Tianjin University of Science and Technology, Tianjin 300457, China

[2] School of Marine Science and Technology, Tianjin University, Tianjin 300072, China

Received 5 December 2020; accepted 22 February 2021

Abstract

Antarctic Bottom Water (AABW) plays an important role in the meridional overturning circulation and contributes significantly to global heat transport and sea level rise (SLR). Based on the Global Ocean (1/12)° Physical Reanalysis (GLORYS12V1) products and conductivity-temperature-depth instrument data from the World Ocean Circulation Experiment hydrographic program, we analyzed the trends in the thickness, volume, temperature, salinity, and neutral density of the AABW in the Amundsen Sea from 1993 to 2017. Over the past 25 years, the volume has decreased by 3.45×10^{12} m^3/a, thinning at a rate of 5 m/a. In the vertical direction, the contraction of the AABW is compensated by the volume expansion of the Circumpolar Deep Water. As the volume of AABW decreases, the temperature of the AABW increases by about 0.002°C/a. This warming is equivalent to a heat flux of 0.27 W/m^2. A local SLR is produced due to thermal expansion of 0.35 mm/a. During the study period, the neutral density decreased by 0.000 3 $kg/(m^3{\cdot}a)$ due to warming. In the horizontal direction, the volume of AABW flowing from the Ross Sea into the Amundsen Sea gradually decreases and the temperature of the AABW increases continuously. The horizontal transport loss of the AABW volume is 4.07×10^{14} m^3 and the horizontal heat transport results in a 0.03°C increase in the temperature of the AABW.

Key words: Antarctic Bottom Water, Amundsen Sea, thickness, volume, hydrographic property

Citation: Bai Yu, Zhao Liang, Xiao Jingen, Lin Shiying. 2022. Contraction and warming of Antarctic Bottom Water in the Amundsen Sea. Acta Oceanologica Sinica, 41(4): 68–79, doi: 10.1007/s13131-021-1829-8

1 Introduction

The Southern Ocean is one of the main components of the world ocean (Carter et al., 2008). Its unique geographic location enables it to be directly connected with other ocean basins and it is a major participant in global freshwater transport and global heat transport (Ganachaud and Wunsch, 2000; Lumpkin and Speer, 2007; Schmittner et al., 2007). It has a large impact on maintaining global ocean circulation, biogeochemical cycling, and Antarctic ice sheet stability (Rintoul, 2018).

Antarctic Bottom Water (AABW), which is widely distributed around the Antarctic, forms by the mixing of the Lower Circumpolar Deep Water (LCDW) rising to the Antarctic continental slope with the cold shelf water (Foster and Carmack, 1976; Jacobs et al., 1985; Orsi et al., 1999). The AABW spreads from south to north in the global deep ocean below 1 000 m, dominating the global deep ocean (Purkey and Johnson, 2010). Current studies show that there are four main sources of AABW: the Weddell Sea, the Ross Sea, the ocean next to Adélie Land, and the area near Cape Darnley (Mantyla and Reid, 1983; Meredith, 2013; Ohshima et al., 2013). The Ross Sea produces 20% of the AABW (Jacobs, 2004). Its main destination is the Southeast Pacific Basin (Jacobs, 2004) where the AABW flows eastward along the Pacific-Antarctic Ridge, filling the Amundsen-Bellingshausen Basin (Purkey et al., 2019).

The polar regions have been significantly affected by global climate change. Relevant studies have shown that changes in the Southern Ocean have not been confined to the surface; intermediate and deep waters are changing as well (Azaneu et al., 2013). The AABW has warmed globally in recent decades, contributing about 10% of recent total ocean heat uptake (Purkey and Johnson, 2012). This warming indicates a global contraction of AABW (Purkey and Johnson, 2012). The thickness and volume of AABW have also decreased. The volume of denser AABW decreased by more than 50% between 1969–1971 and 2008–2012, and AABW thinned more than 100 m per decade (van Wijk and Rintoul, 2014). The volume of AABW was significantly reduced in the Southern Ocean and in the meridional overturning circulation between the 1980s and 2000s at a loss rate of 8.2 (±2.6)$\times10^6$ m^3/s (Purkey and Johnson, 2012). Furthermore AABW contracted to varying degrees in different basins in the Southern Ocean (Purkey and Johnson, 2012). The Weddell Sea Bottom Water also has warmed (+0.01°C/a) during 1989–1995 (Azaneu et al., 2013). The Princess Elizabeth Trough and the Australia-Antarctic Basin have warmed by 0.05°C and 0.1°C, respectively, during 1994/1995–2007 (Johnson et al., 2008a). Between the 1990s and 2000s, areas below 4×10^7 Pa in the Weddell-Enderby Basin, Australia-Antarctic Basin, and Southeast Pacific Basin have warmed by 0.33 W/m^2, 0.24 W/m^2, and 0.15 W/m^2, respectively (Purkey and Johnson, 2010). Between 1970 and 2012, the warming signal in the Australian-Antarctic Basin increased with increasing distance downstream along the AABW pathway, with a rate of 0.02°C per decade near the source (140°E and 150°E), a rate of 0.03°C per

Foundation item: The Impact and Response of Antarctic Seas to Climate Change Program under contract No. RFSOCC2020-2022-No. 18; the National Key Research and Development Program of China under contract No. 2016YFA0601301.
*Corresponding author, E-mail: zhaoliang@tust.edu.cn

decade near 115°E and 84°E, and a rate of 0.04°C per decade near the south of mid-ocean ridge (80°E and 115°E) (van Wijk and Rintoul, 2014).

The Amundsen Sea is located in the Pacific sector of the Southern Ocean, downstream of the Ross Sea (Koshlyakov and Tarakanov, 2003; Ozaki et al., 2009). In this area, AABW originates mainly from the Ross Sea (Orsi et al., 1999; Koshlyakov and Tarakanov, 2003; Uenzelmann-Neben and Gohl, 2012). The AABW in the Amundsen Sea flows following the path of the Antarctic Circumpolar Current (ACC) into the Amundsen–Bellingshausen Basin (Orsi et al., 1999). After circulating in the deep basin, the bottom water flows northward through deep fracture zones along the Pacific-Antarctic Ridge into the Southwest Pacific Basin and continues northward into the Pacific Basin along the deep western boundary current (Reid, 1997; Lumpkin and Speer, 2007; Johnson, 2008; Purkey and Johnson, 2012). Following the pathway of the AABW, the abyssal Amundsen–Bellingshausen Basin and the abyssal Southwest Pacific Basin have warmed by 0.17 W/m^2 and 0.12 W/m^2, respectively (Purkey et al., 2019). Subsequently, the contraction of the volume of the AABW was found along the pathway in the lower limb of the meridional overturning circulation (Purkey and Johnson, 2012). The AABW provides the source of the coldest water involved in the global meridional redistribution of heat (Orsi et al., 2002), which is the densest water in the global overturning circulation (Meredith et al., 2011). The warming and volume loss were interpreted as a global slowdown of the bottom limb of the meridional overturning circulation (Johnson et al., 2008b; Purkey and Johnson, 2012). Insufficient attention has been paid to AABW in the Amundsen Sea, most likely because the Amundsen Sea itself forms little of the AABW (Foster and Carmack, 1976; Orsi et al., 1999). However, variations in the AABW have important implications for global heat transport and sea level rise (SLR), and the formation, circulation, and variability of the AABW deserves further exploration (Purkey and Johnson, 2010; Purkey et al., 2018, 2019). Therefore, a deeper exploration of the variability of AABW properties in this region is needed. The remote location of the Amundsen Sea, which is typically a data-poor region (Meredith et al., 2016), makes it difficult to perform a long-term continuous analysis of AABW in the Amundsen Sea. In this paper, the Global Ocean (1/12)° Physical Reanalysis (GLORYS12V1) products was used to analyze and inform discussion of the variations in the AABW in the Amundsen Sea.

2 Data and methods

The main study area of this paper is the Amundsen Sea. Its geographic extent and bathymetric distribution are shown in Fig. 1. The AABW in the Amundsen Sea is distributed mainly in the Pacific deep basins. Its source water comes primarily from the Ross Sea. From the Ross Sea, the AABW flows eastward along the Pacific-Antarctic Ridge, through the cyclonic circulations of the major subpolar gyres, along the path of the ACC, and into the Amundsen Sea (Orsi et al., 1999; Koshlyakov and Tarakanov, 2003; Purkey et al., 2019).

2.1 *Data*

GLORYS12V1—GLOBAL_REANALYSIS_PHY_001_030 is based on the Copernicus Marine Environment Monitoring Service system ((1/12)° horizontal resolution and 50 vertical levels). It uses version 3.1 of Nucleus for European Modelling of the Ocean (Jackson et al., 2019). Its atmospheric forcing uses interim European Centre for Medium-Range Weather Forecasts Re-Analysis (ERA-Interim) (Jackson et al., 2019). Using a reduced-order Kalman filter, GLORYS12V1 assimilates a variety of data, including along-track altimeter data, satellite sea surface temperature, sea ice concentration, and *in situ* temperature and salinity vertical profiles. A three-dimensional variational (3D-VAR) scheme corrects for large-scale biases that can develop in slowly evolving temperature and salinity (Nardelli, 2020).

The publicly available conductivity-temperature-depth (CTD) instrument data used in this paper are from the World Ocean Circulation Experiment Hydrographic Program supported by the Clivar & Carbon Hydrographic Data Office. The dataset used in this study is composed of two repeated sections: P18 (purple dots) and S04P (orange dots) (Fig. 1). The occupation dates of P18 are 1994, 2007, and 2016, and for S04P are 2011 and 2018. Since GLORYS12V1 is not complete in 2018, this study covers the period from 1993 to 2017. Only part of GLORYS12V1 in 2018 was used when compared with CTD in S04P.

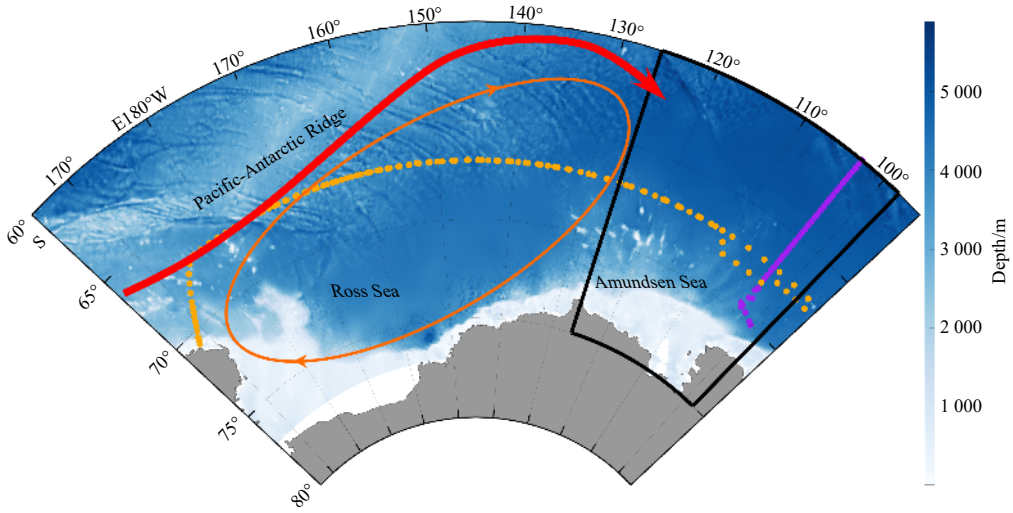

Fig. 1. The bathymetry and station locations in the main study area, with purple dots for the P18 (including 1994, 2007, and 2016), yellow dots for the S04P (including 2011 and 2018), and the Amundsen Sea within the black box. The red and orange arrows represent the schematic pathway of the Antarctic Bottom Water and Ross Gyre, respectively.

2.2 *Methods*

The AABW is commonly distributed in the deep ocean (Orsi et al., 1999; Carter et al., 2008). In order to calculate the thickness of the AABW more accurately, this study linearly interpolated the temperature and salinity data of GLORYS12V1 and CTD from the surface to the bottom with an interpolation interval of 1 m. To better characterize AABW, it is defined by a neutral density (γ^n) (Orsi et al., 1999). In this paper, the isopycnal (γ^n=28.27 kg/m^3) was defined as the upper boundary of the AABW. The distance between the upper boundary of the AABW and the seabed was defined as the thickness of the AABW. Variations in the volume, temperature, salinity, and neutral density of the AABW within this thickness range were analyzed. To further explore the compensation of the contraction of the AABW, different neutral densities were also used to define the Circumpolar Deep Water (CDW, 28.00 kg/m^3$\leqslant\gamma^n$<28.27 kg/m^3) (Whitworth III et al., 1985) and the Antarctic Surface Water (AASW, γ^n<28 kg/m^3) (Orsi and Wiederwohl, 2009), and to discuss the role of the expansion of several water masses in compensating for the contraction of the AABW. The local heat flux (Q) and steric SLR (F) were estimated based on the variations in volume and temperature of the AABW in the Amundsen Sea. Equations (1) and (2) are from Purkey and Johnson (2010):

$$Q=\left[\frac{1}{a\,(\mathrm{AABW})}\right]\int_{\mathrm{top}}^{\mathrm{bottom}}\rho C_p\left(\frac{\mathrm{d}\theta}{\mathrm{d}t}\right)a\mathrm{d}z, \tag{1}$$

$$F=\left[\frac{1}{a\,(\mathrm{AABW})}\right]\int_{\mathrm{top}}^{\mathrm{bottom}}\alpha\left(\frac{\mathrm{d}\theta}{\mathrm{d}t}\right)a\mathrm{d}z, \tag{2}$$

where θ, t, z, ρ, C_p, α, and a denote potential temperature, time, depth, density, specific heat, thermal expansion coefficient, and the surface area of each depth, respectively. C_p and α were calculated using the temperature and salinity in GLORYS12V1 by Thermodynamic Equation of Seawater (TEOS-10), respectively. The difference from the equation of Purkey and Johnson (2010) is that in this paper a(AABW) represents the total surface area of the AABW in the Amundsen Sea. The a (AABW) was calculated by adding all the grid areas covered by AABW in the Amundsen Sea in GLORYS12V1. In the equation, "top" denotes the upper boundary of the AABW and "bottom" denotes the seafloor. The volume transport (V) and heat transport (H) through the Amundsen Sea at the three boundary sections (126°W, 98°W, and 60°S) were calculated using the following equations:

$$V=\sum A\upsilon_{\mathrm{n}}, \tag{3}$$

$$H=\sum\rho C_pA\upsilon_{\mathrm{n}}\left(T-T_{\mathrm{ref}}\right), \tag{4}$$

where A denotes the area of a single grid on the boundary section, υ_{n} denotes the normal velocity component on a single grid, T denotes the temperature on a single grid, and T_{ref} denotes the average temperature of the AABW in the Amundsen Sea in different years.

2.3 *Validation*

As shown in Fig. 2, the distribution of the AABW in the P18 was almost identical in both GLORYS12V1 and CTD sections. Near 65°S, the depth of the AABW upper boundary was shallower than 4 000 m in 1994, was roughly at 4 000 m in 2007, and deeper than 4 000 m in 2016, with the position of the AABW upper boundary sinking over this period. The average depth of the AABW upper boundary on the CTD section was 4 119 m in 1994, 4 142 m in 2007, and 4 254 m in 2016, sinking by an average of 2 m/a between 1994 and 2007, and by an average of 12 m/a between 2007 and 2016. This trend in the position of the AABW upper boundary also occurred in the GLORYS12V1 section, with average depths of 4 059 m, 4 072 m, and 4 157 m in 1994, 2007, and 2016, respectively. From 1994 to 2007, the average sinking rate was 1 m/a, and from 2007 to 2016, the average sinking rate was 9 m/a. The P18 shows that the thickness of the AABW decreased continuously with time in the longitudinal direction.

In the S04P section (Fig. 3), there was a descending trend in the position of the upper boundary of the AABW between 2011 and 2018. In the CTD section, there was a general deepening of the position of the upper boundary of the AABW from 180° to 110°W and from 100°W to 90°W. The average depth east of 180° deepened from 3 176 m to 3 237 m with a sinking rate of 9 m/a. This descending trend was more pronounced in the GLORYS12V1 section, where the average depth east of 180° deepened from 2 955 m to 3 208 m, with a sinking rate of 36 m/a. This trend of decreasing thickness in the latitudinal direction could be seen in the S04P section.

The sinking of the upper boundary of the AABW in the P18 and S04P was accompanied by an increase in the temperature of the AABW (Figs 2 and 3). In the P18 section, 0°C isotherms were present in both GLORYS12V1 and CTD sections in 1994. All 0°C isotherms disappeared in 2007. From 1994 to 2016, the proportion of water with a temperature lower than 0.08°C correspondingly decreased. This trend was more dramatic in GLORYS12V1, where in 2016, 0.08°C isotherms were present between 65°S and 60°S. In the S04P section, the easternmost 0°C isotherm in the 2011, CTD section was 115°W, and by 2018, the easternmost 0°C isotherm was near 130°W. This latitudinal warming trend was also present in the GLORYS12V1 section, where cold water with temperatures below 0.08°C reached eastward to 100°W in 2011 and to 110°W in 2018. In the P18 and S04P sections, there were some differences in the salinity between the two datasets. In the CTD sections, the salinity showed a freshening trend in the deep ocean, while in the GLORYS12V1 section this trend was reversed. However, the variation in salinity is relatively weak compared to those of temperature and neutral density. The warming trends in the P18 and S04P sections were accompanied by a decline in the neutral density of the AABW. In the P18 section, the 28.3 kg/m^3 isopycnal was gradually sinking and disappearing. Warming in the temperature was likely the major factor driving the neutral density changes (Azaneu et al., 2013).

3 Results and discussion

The properties of AABW in the Amundsen Sea are changing in thickness, volume, temperature, salinity, and neutral density. This paper analyzed the above variations of the AABW in the Amundsen Sea from 1993 to 2017 based on GLORYS12V1. We also discuss the effects of the volume expansion of several other lighter water masses and the volume transport and heat transport at the boundary sections.

3.1 *Variations in thickness and volume of the AABW in GLORYS12V1*

The average thickness of the AABW from 1993 to 2017 is shown in Fig. 4a. During this period, it was thinner on the side near the Antarctic continent, thicker in the middle of the Ross

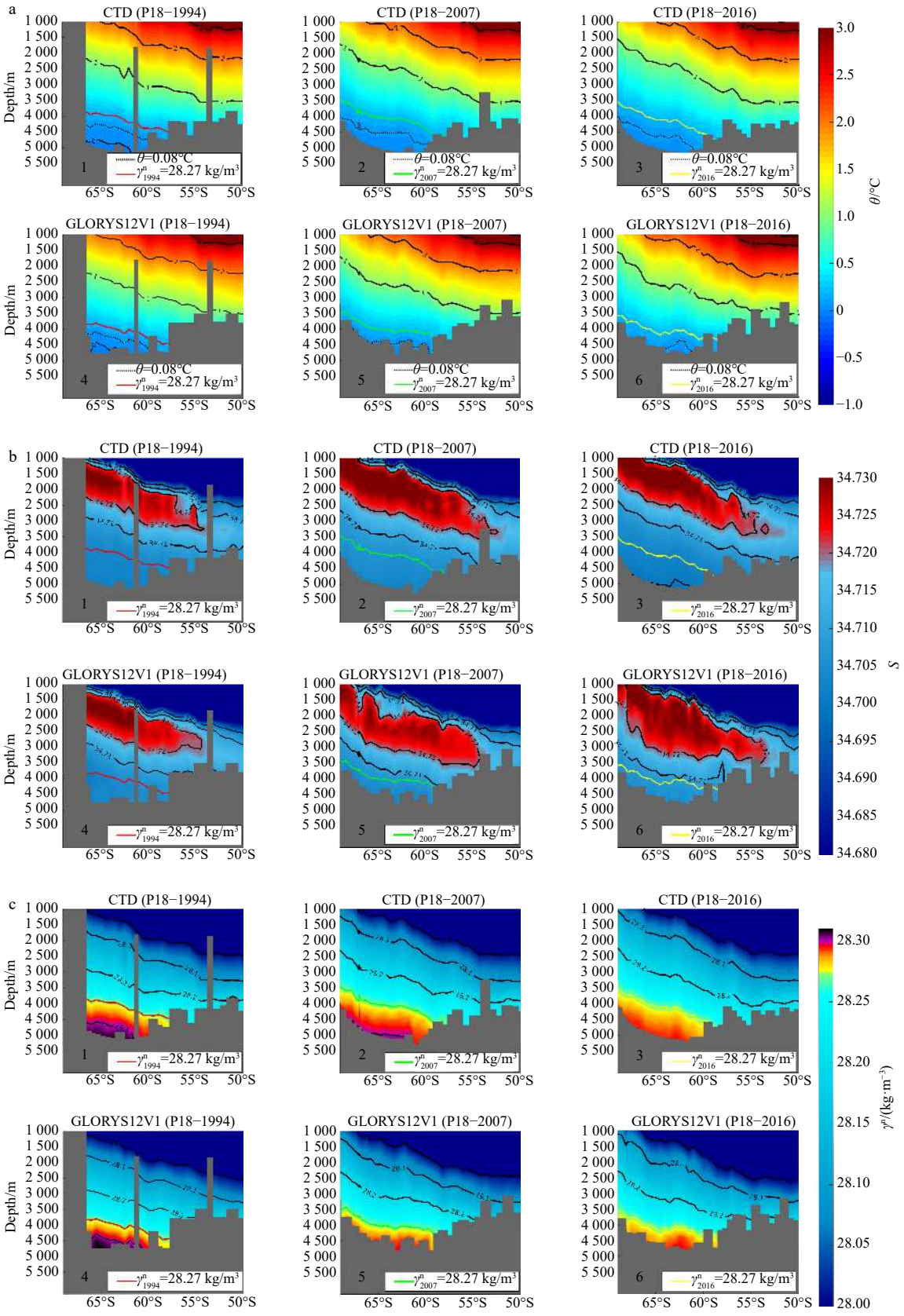

Fig. 2. Comparison of conductivity temperature depth (CTD) section with GLORYS12V1 section in the P18, where the black solid line represents the contour; the black dashed line in a represents the 0.08°C contour; the red solid line represents the 1994 Antarctic Bottom Water (AABW) upper boundary position; the green solid line represents the 2007 AABW upper boundary position; and the yellow solid line represents the 2016 AABW upper boundary position. a, b, and c show the temperature (θ), salinity (S), and neutral density (γ^n) comparisons, respectively.

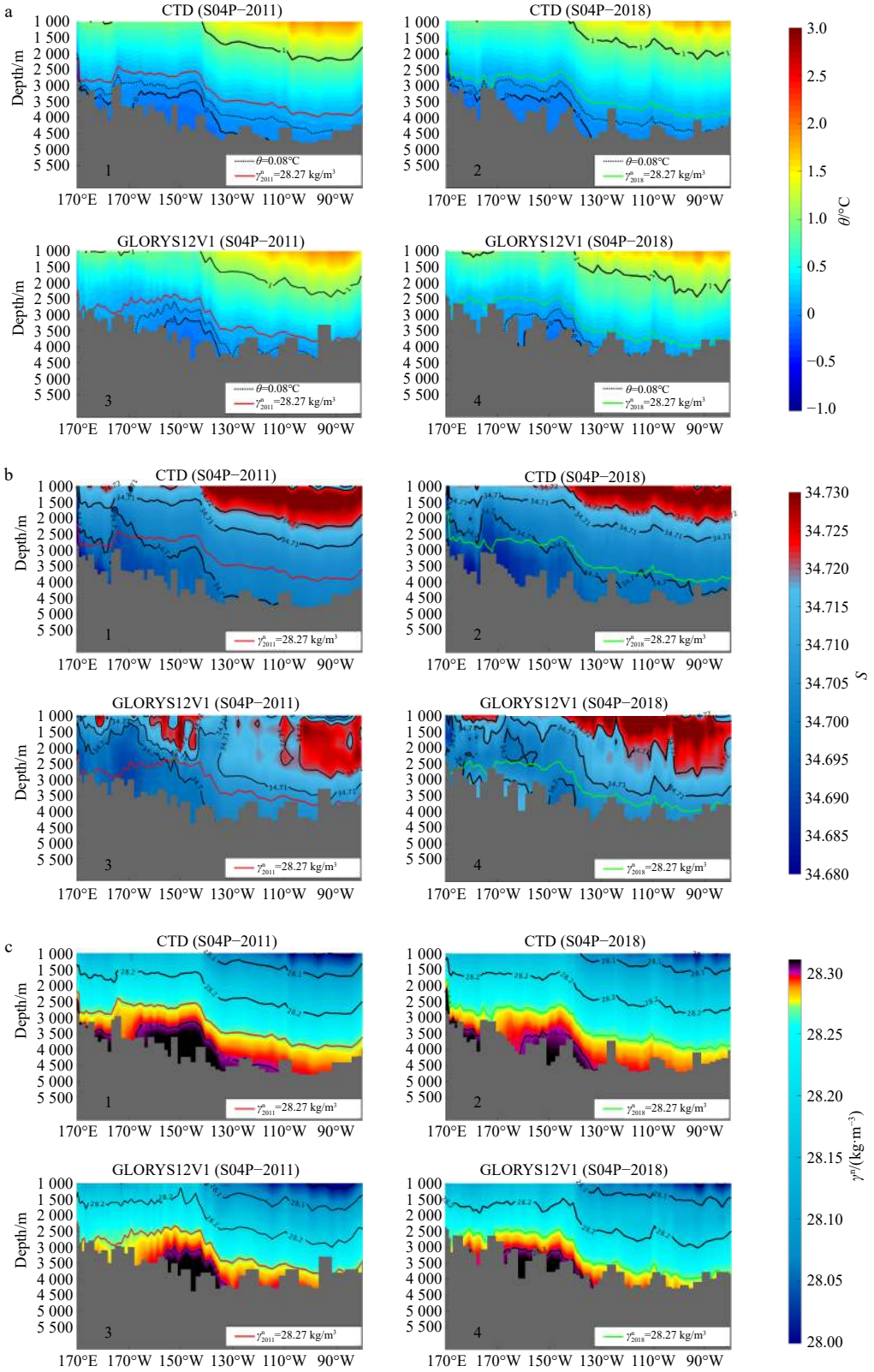

Fig. 3. Comparison of conductivity temperature depth (CTD) section with GLORYS12V1 section in the S04P, where the black solid line represents the contour, the black dashed line in a represents the 0.08°C contour; the red solid line represents the 2011 Antarctic Bottom Water (AABW) upper boundary position; and the green solid line represents the 2018 AABW upper boundary position. a, b, and c show the temperature (θ), salinity (S), and neutral density (γ^n) comparisons, respectively.

Sea, and thinned gradually from the center to the periphery. In the Amundsen Sea, the thickness of the AABW ranged between 200 m and 1 300 m, with a maximum value of about 1 879 m. The AABW in the Amundsen Sea was relatively thin in a large region

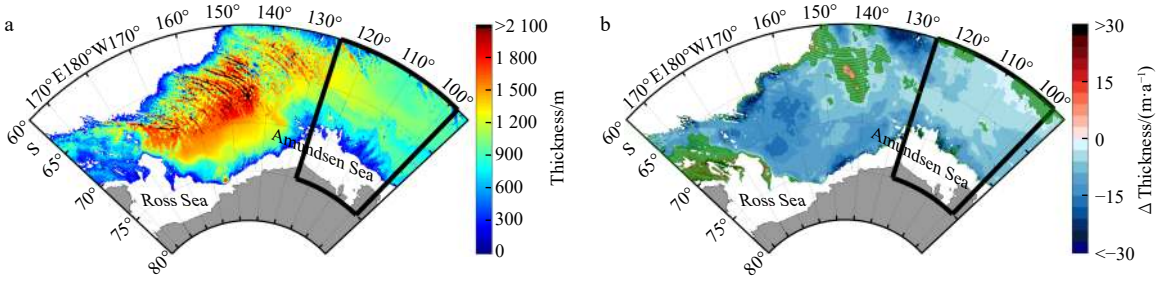

Fig. 4. The average thickness of the Antarctic Bottom Water (AABW) (a) and average thickness variation of the AABW (b) from 1993 to 2017. The green range in b represents the area where the trend is not statistically significant at the 95% confidence level (same as in Figs 7b, 7d and 9b).

near the Antarctic continent, and relatively thick on the northwestern side of the Amundsen Sea. The AABW became thinner as it moved from the Ross Sea to the Amundsen Sea (Orsi et al., 1999; Koshlyakov and Tarakanov, 2003; Ozaki et al., 2009). The AABW was thicker in the Ross Sea than in the Amundsen Sea. Most areas were more than 1 200 m, a few areas more than 2 100 m, with a maximum value of about 2 860 m.

The variation in the average thickness of AABW from 1993 to 2017 is shown in Fig. 4b. The Amundsen Sea showed a predominantly decreasing trend in thickness, which was statistically significant in most areas. This trend was synchronized in the southeastern Pacific and could be traced back to the source of the AABW, the Ross Sea, where it is more dramatic. Thickness decreased by more than 30 m/a in parts of the Ross Sea, but an upward trend existed west of 140°W.

To further analyze the interannual variations in thickness, regression analysis (Fig. 5a) was performed for the statistically significant areas in Fig. 4b. In the Amundsen Sea, the AABW thickness showed a fluctuating decreasing trend from 1993 to 2017 (Fig. 5a). For example, between 1995 and 2002, the AABW thickness decreased from 1 024 m to 946 m by 11 m/a; between 2005 and 2007, the AABW thickness decreased from 974 m to 923 m by 26 m/a; and between 2011 and 2016, the AABW thickness decreased from 944 m to 853 m by 18 m/a. Although there were periods in which the thickness of the AABW in the Amundsen Sea increased, overall the thickness, decreased by an average of 5 m/a from 1993 to 2017, with a maximum decrease of 35 m between 2006 and 2007. In the Ross Sea, the thickness of the AABW decreased from 1 307 m to 1 106 m between 1994 and 2012 by 11 m/a and from 1 117 m to 1 089 m between 2013 and 2017 by 7 m/a. The thickness of the AABW in the Ross Sea also did not decrease monotonically, but overall it decreased by an average 10 m/a from 1993 to 2017.

In the latitudinal direction (Fig. 5b), the thickness of the AABW in the Amundsen Sea fluctuated between 723 m and 1 138 m, decreasing and then increasing from west to east. It had a maximum thickness near 125°W and a minimum thickness near 107.5°W. In the longitudinal direction (Fig. 5c), the thickness of the AABW in the Amundsen Sea fluctuated between 73 m and 1 139 m. It was lowest south of 70°S, increased, and then decreased in thickness from 70°S to 60°S. This variation in the thickness of the AABW is due to a decrease in the rate of formation and variation in its properties (van Wijk and Rintoul, 2014). The lighter deep water produced by the freshening of the cold shelf

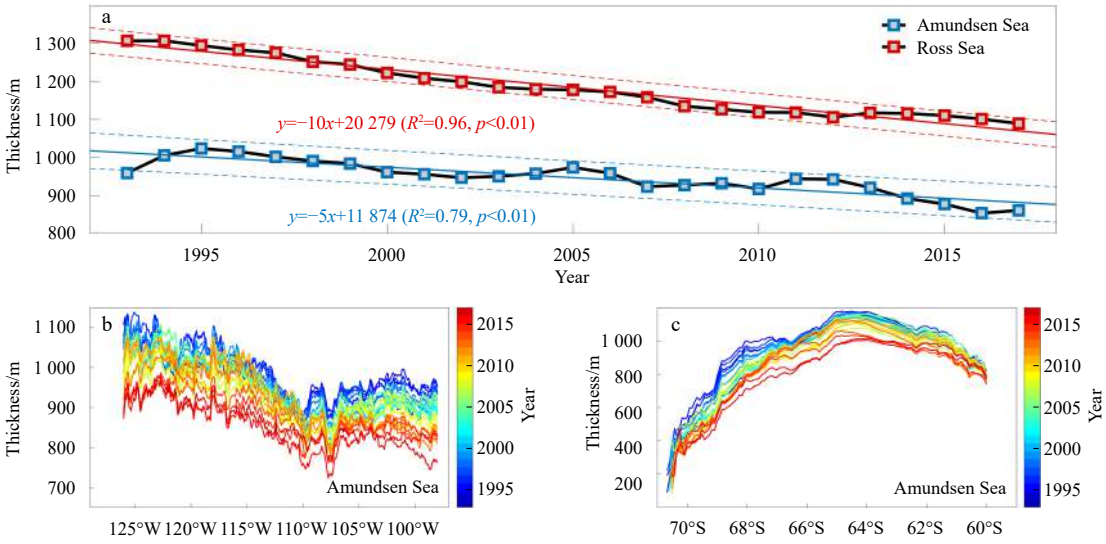

Fig. 5. The annual variation of the thickness in the Antarctic Bottom Water (AABW). In a, blue squares indicate the thickness in the Amundsen Sea and red squares indicate the thickness in the Ross Sea. R^2 and p in a denote the coefficient of determination and the statistical p value (same as in Figs 6, 8a, 8d, 10a and 11). b. The latitudinal annual variation in the thickness of the AABW in the Amundsen Sea was derived by meridional mean. c. The longitudinal annual variation in the thickness of the AABW in the Amundsen Sea was derived by zonal mean. The different colors in b and c represent different years.

water is an important factor in the reduction of AABW volume and the output of lighter water to the world ocean (Azaneu et al., 2013), which then gradually affects downstream areas along the pathway of the AABW (Orsi et al., 1999; Kawano et al., 2006; Johnson et al., 2014).

The decrease in the thickness of the AABW in the Amundsen Sea was accompanied by a corresponding variation in volume (Fig. 6). The contraction of the AABW was compensated by an increase in the volume of the lighter water mass (van Wijk and Rintoul, 2014). Between 1995 and 2002, the volume of AABW decreased from 6.33×10^{14} m^3 to 5.89×10^{14} m^3 at a rate of 6.28×10^{12} m^3/a. Although the volume of AABW increased during some years, that did not affect the overall decreasing trend. Between 2011 and 2017, the volume of AABW decreased from 5.85×10^{14} m^3 to 5.34×10^{14} m^3, at a rate of 8.57×10^{12} m^3/a. Over the entire period, the volume of AABW decreased by 6.75×10^{13} m^3 at a rate of 3.45×10^{12} m^3/a. Over the same period, the volume of the CDW increased by a total of 1.10×10^{14} m^3 and the AASW decreased by 4.24×10^{13} m^3. From 1993 to 2017, the contraction of the volume of the AABW was compensated by the expansion of the CDW. The volume loss of cold AABW corresponds to the deepening of isotherms. The temperature class of water compensating for this deep loss is in the temperature range of CDW (Purkey et al., 2019).

3.2 *Variations in temperature, salinity, and neutral density of the AABW in GLORYS12V1*

As shown in Fig. 7a, the average temperature of the AABW in the Amundsen Sea from 1993–2017 was 0.04–0.22°C. Higher temperatures were near the onshore side and temperature decreased gradually from south to north. The temperature of the AABW in the Ross Sea, located in the upstream of the Amundsen Sea, was significantly lower. There was a low-value region with a temperature less than 0°C in the central region. In the pathway from the Ross Sea to the Amundsen Sea, the temperature gradually increased. As shown in Fig. 7b, the AABW in the Amundsen Sea exhibited a warming signal with a few non-statistically significant areas. The AABW also showed a warming signal over most of its range in the Ross Sea, with only a portion of its range (160°–170°W) showing a cooling signal. Observations of several hydrographic sections crossing the South Pacific Ocean have also revealed steady to accelerated bottom water warming since the 1990s (Purkey et al., 2019). The average salinity distribution of the AABW (Fig. 7c) was mostly consistent with the temperature, and that of the Amundsen Sea was significantly higher than that of the Ross Sea. There were more areas with non-statistically significant trends in salinity than in temperature and thickness. In the Amundsen Sea, the salinity of the AABW increased significantly. However, a freshening trend in the AABW has been found near the eastern Ross Sea (150°–175°W). This trend has been linked to a decrease in salinity of the high salinity shelf water in the Ross Sea (Jacobs et al., 2002; Jacobs and Giulivi, 2010).

From 1994 to 2002, the temperature of the AABW in the Amundsen Sea exhibited a monotonic increase from 0.069°C to 0.090°C at a rate of approximately 0.003°C/a. Between 2007 and 2011 there was a large fluctuation (Fig. 8a). The monotonically increasing trend resumed during the period from 2011 to 2017, increasing from 0.097°C to 0.122°C at a rate of approximately 0.004°C/a. The average temperature increased over the entire period of 1993–2017 was 0.002°C/a. The temperature of the AABW in the Ross Sea was lower than in the Amundsen Sea during the same period (the same year), but there was also a rising trend over time that was even more significant than the trend in the Amundsen Sea. Observations have shown that the abyssal warming below 4 000 m is associated with a bottom-intensified descent of the deepest isotherms, with stronger warming in the Ross Sea than in the Amundsen Sea (Purkey et al., 2019). There is a significant correlation between the temperature of the AABW in the Ross Sea and the temperature of the AABW in the Amundsen Sea (correlation coefficient R of 0.95). Although the salinity of the AABW increased in both the Ross Sea and the Amundsen Sea (Fig. 8d), there were areas of statistically significant salinity reduction in the Ross Sea (Fig. 7d).

In the latitudinal direction (Figs 8b, e), the west side of the Amundsen Sea was significantly cooler in 1993, with a minimum temperature of less than 0.05°C. In most years, the temperature decreased from 126°W to 117.5°W and increased from 117.5°W to 107.5°W. The salinity was generally lower and higher in 1993 and 2017, respectively, than in other years. From 1999 to 2015, the salinity changes were more consistent, increasing from west to east.

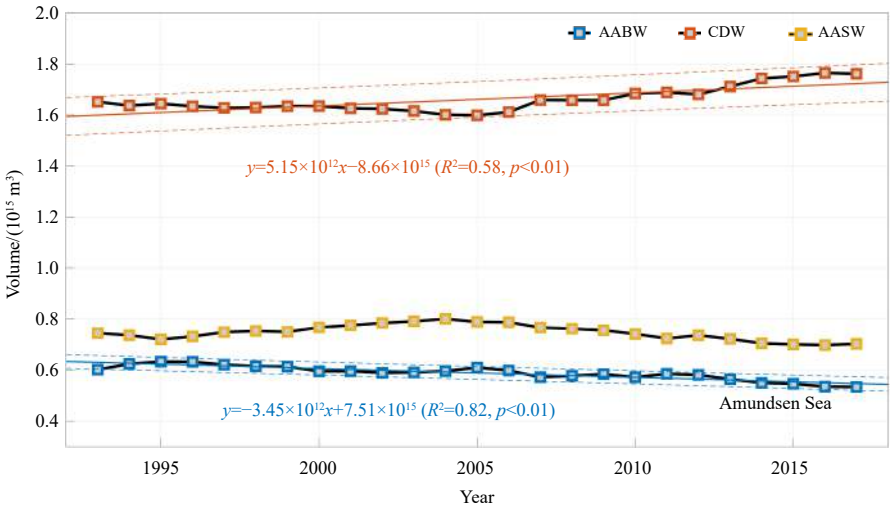

Fig. 6. The annual variation in the volume of the three water masses in the Amundsen Sea. Blue squares represent the Antarctic Bottom Water (AABW), red squares represent the Circumpolar Deep Water (CDW), yellow squares represent the Antarctic Surface Water (AASW).

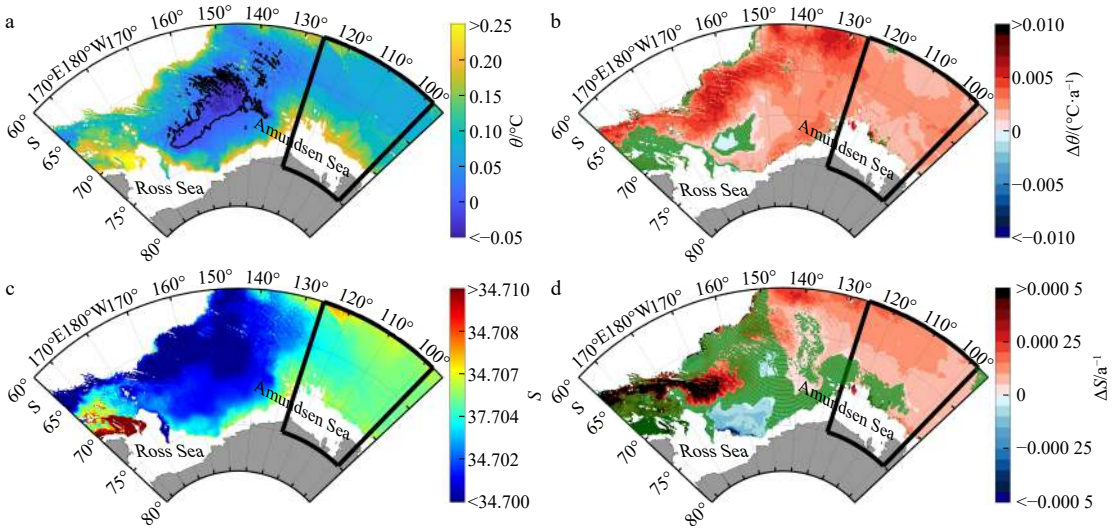

Fig. 7. The average temperature of the Antarctic Bottom Water (AABW) (a) and average temperature variation of the AABW (b) from 1993 to 2017. The Amundsen Sea is within the black box. The black solid line in a indicates the 0°C contour. c, d are same as a and b but for salinity.

In the longitudinal direction (Figs 8c, d), the variation in temperature was more regular, with a general decrease in temperature from 70°S to 66°S and a gradual increase in temperature from 66°S to 60°S. In 1993, the salinity was lower in the southern Amundsen Sea; while in 2017, the salinity was higher in the northern Amundsen Sea. From 1999 to 2016, the salinity initially decreased and then increased from south to north. In both latitudinal and longitudinal directions, the variations in temperature from 1993 to 2017 showed a warming signal.

In the context of this general warming of the deep ocean (Johnson and Doney, 2006; Kawano et al., 2006; Masuda et al., 2010; Patara and Böning, 2014; Zanowski et al., 2015), the bottom of the Amundsen Sea is also warming, with the AABW warming by 0.002°C/a. This warming is equivalent to a heat flux of 0.27 W/m^2. It also produces a local SLR due to thermal expansion of 0.35 mm/a. Upstream of the Amundsen Sea, the Ross Sea has a greater degree of heat flux and local SLR, which are 0.39 W/m^2, 0.43 mm/a, respectively.

As shown in Fig. 9a, the average neutral density distribution of the AABW was mostly opposite that of the temperature, and that of the Amundsen Sea was significantly lower than that of the Ross Sea. In the low-temperature region, the AABW was dense. For example, the region where the temperature was less than 0°C (Fig. 7a) corresponded to the region where the neutral density was greater than 28.305 0 kg/m^3. As shown in Fig. 9b, the AABW in the Amundsen Sea exhibited a statistically significant decrease in neutral density. This trend is linked to the temperature changes, with the neutral density decreasing in the warming regions. Correspondingly, an increasing trend in neutral density was found in the cooling region of the Ross Sea.

From 1993 to 2017, the neutral density of the AABW in the Amundsen Sea exhibited decreased from 28.292 2 kg/m^3 to 28.285 9 kg/m^3 at a rate of 0.000 3 kg/(m^3 ·a) (Fig. 10a). However, no statistically significant trend was found in the Ross Sea. In the open ocean, warming is the major contributor to decreases in the neutral density of the AABW (Azaneu et al., 2013). The neutral density can be seen to vary opposite to the temperature trend in both the longitudinal and latitudinal directions (Figs 10b, 10c, 8b, 8c). As the temperature increased, the neutral density gradually decreased. There was a significant negative correlation between the temperature and neutral density of the AABW in the Amundsen Sea (correlation coefficient R of –0.98).

3.3 *Variations in volume transport and heat transport of the AABW in GLORYS12V1*

Several previous studies have shown two important variations in contraction and warming of the AABW (Purkey and Johnson, 2010; Meredith et al., 2011; Shimada et al., 2012; Johnson et al., 2014; Purkey et al., 2019). In this study, the thickness and volume of the AABW in the Amundsen Sea show obvious decreasing trends. From 1993 to 2017, the thickness decreased by 5 m/a, while at the same time the volume decreased by 3.45×10^{12} m^3/a. Since the Amundsen Sea does not form the AABW, this trend is influenced by the upstream aspects. The southern end of the Amundsen Sea connects to the Antarctic continent, so only the volume transport at the remaining three boundaries of the Amundsen Sea was calculated (Fig. 11a). Through the 126°W section, AABW continuously flows from the Ross Sea to the Amundsen Sea, and the volume transport has been gradually decreasing in a fluctuating downward trend from 1993 to 2017, implying a gradual decrease in the volume of AABW delivered from the source (Ross Sea) to the Amundsen Sea. In most years, the AABW flows out of the Amundsen Sea from sections 98°W and 60°S. The total volume transport (ΔV) of the three boundaries shows that the total volume transport (ΔV) is less than 0 in all years. There is a deficit in the horizontal (advection) direction for each year of the AABW volume transport. The total volume losses at all three boundaries is 4.07×10^{14} m^3 during the period 1993–2017. The high salinity LCDW subducts and mixes with the AABW, causing the local salinity to rise (elevating the isopycnal) and compensating for the volume change. While the AABW contracts, the CDW compensates for the loss of bottom water through volume expansion.

From 1993 to 2017, the contraction of the AABW in the Amundsen Sea was accompanied by a temperature variation with an average increase of approximately 0.002°C/a. Geothermal energy is unlikely to be the source of this temperature variation (Purkey et al., 2019). These variations in the properties of the AABW can be traced back to variations in the AABW formation regions (van Wijk and Rintoul, 2014). The warming down-

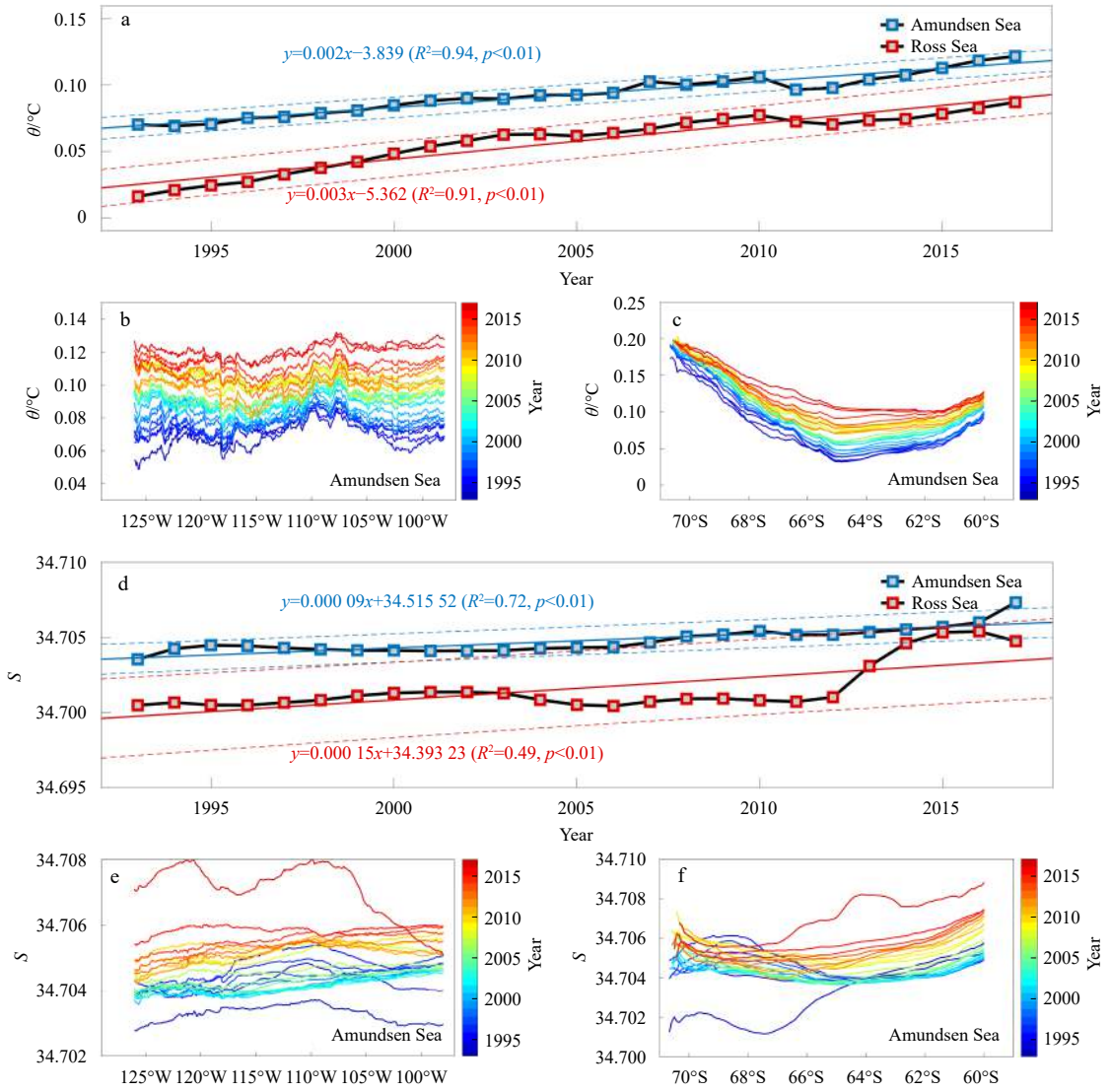

Fig. 8. The annual variations of the temperature and salinity in the Antarctic Bottom Water (AABW). In a, blue squares represent the temperature in the Amundsen Sea and red squares represent the temperature in the Ross Sea. b. The latitudinal annual variation in the temperature of the AABW in the Amundsen Sea was derived by meridional mean. c. The longitudinal annual variation in the temperature of the AABW in the Amundsen Sea was derived by zonal mean. The different colors in b and c represent different years. d–f are same as a–c but for salinity.

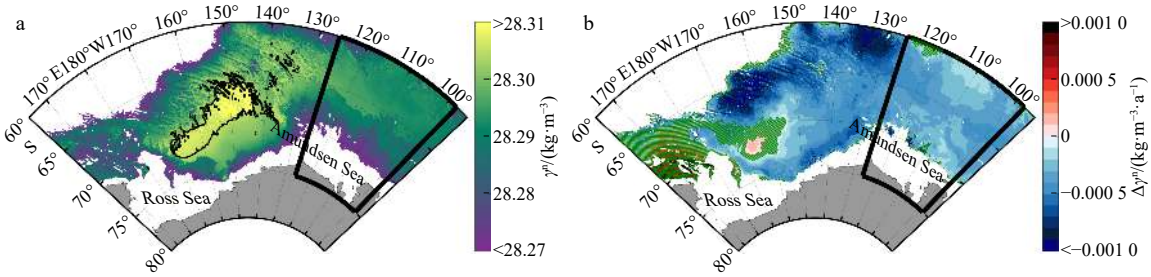

Fig. 9. The average neutral density of the Antarctic Bottom Water (AABW) (a) and the average neutral density variation of the AABW (b) from 1993 to 2017. The black solid line in a indicates the 28.305 0 kg/m^3 contour.

stream of the source (Purkey and Johnson, 2010) reflects a combination of two processes (van Wijk and Rintoul, 2014): the descent of the isopycnals is caused by the contraction of dense water (Purkey and Johnson, 2010) and stratification and mixing changes due to source water freshening (Meredith et al., 2011). Since the freshening of the Ross Sea Bottom Water increases the buoyancy of these waters, it may also decrease the formation rate of the AABW (Purkey et al., 2019). These variations are rapidly

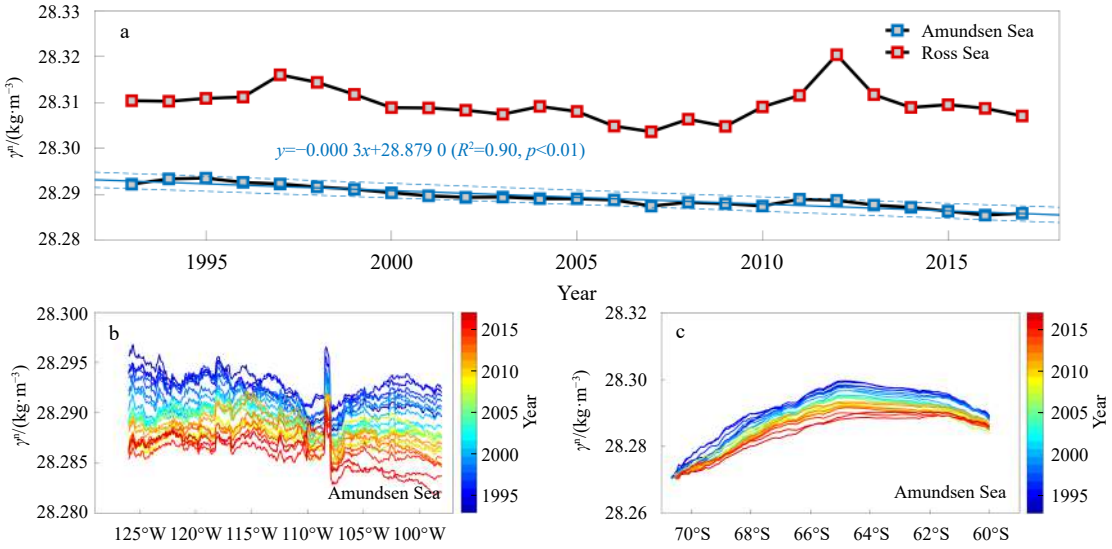

Fig. 10. The annual variation of the neutral density in the Antarctic Bottom Water (AABW). In a, the blue squares represent the neutral density in the Amundsen Sea and the red squares represent the neutral density in the Ross Sea. b. The latitudinal annual variation in the neutral density of the AABW in the Amundsen Sea was derived by meridional mean. c. The longitudinal annual variation in the neutral density of the AABW in the Amundsen Sea was derived by zonal mean. The different colors in b and c represent different years.

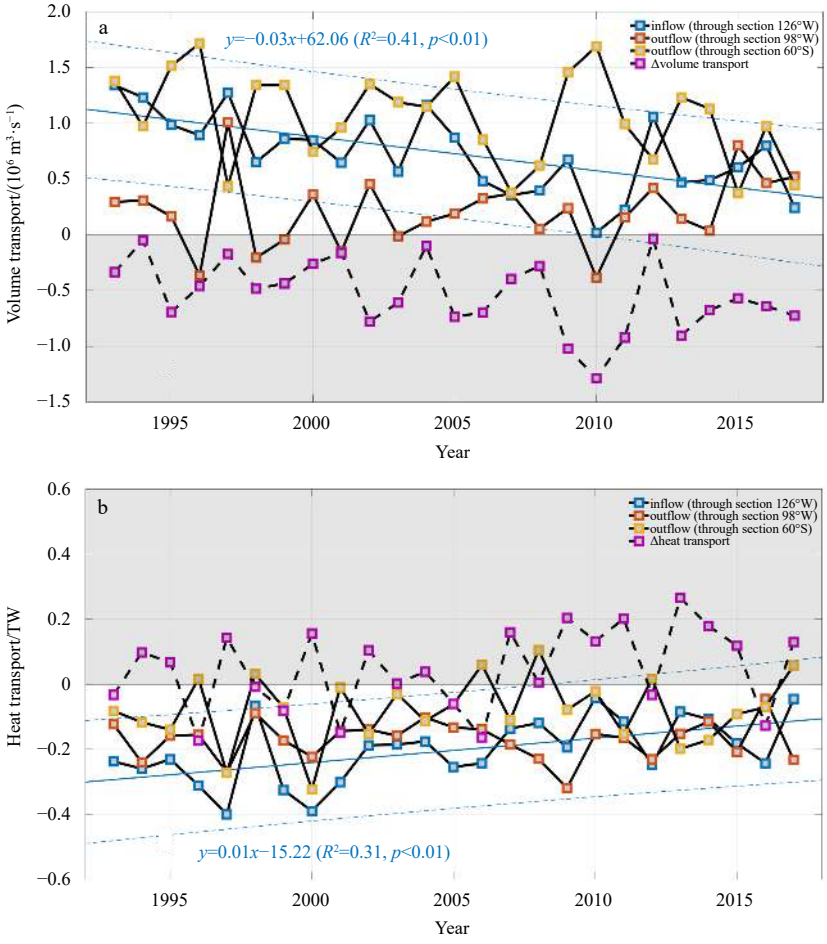

Fig. 11. Volume transport (a) and heat transport (b) in the three boundary sections of the Amundsen Sea. Blue squares indicate the inflow into the Amundsen Sea through 126°W, red squares indicate the outflow from the Amundsen Sea through 98°W, yellow squares indicate the outflow from the Amundsen Sea through 60°S, and purple squares indicate the sum of the transport (total transport) in the three sections. The shaded area in a indicates a volume transport less than 0 m^3/s and the shaded area in b indicates a heat transport more than 0 TW.

propagated through planetary waves to the adjacent deep ocean basin (Masuda et al., 2010). The warming of the deep Southern Ocean is at least partly caused by warm water advection from the source (Purkey and Johnson, 2010). This warming signal is also occurring and more pronounced in the Ross Sea, the upstream source of the AABW in the Amundsen Sea. The AABW in the Ross Sea is cooler than in the Amundsen Sea. The colder AABW flowing into the Amundsen Sea through the 126°W section decreases and warms over time during the inflow. The heat transport through 126°W also shows an upward trend (Fig. 11b), increasing by about 0.01 TW/a. The sum of the heat transport across the three sections contributed to an increase in the temperature of the AABW by approximately 0.03°C and to an increase in the temperature of the AABW in the advection during the period 1993–2017.

4 Conclusions

In this paper, the upper boundary of the AABW in the Amundsen Sea was defined by neutral density, and the trends in the thickness, volume, temperature, salinity, and neutral density of the AABW in GLORYS12V1 and CTD (P18 and S04P) were analyzed. In the vertical direction, compensation for the AABW contraction was estimated using the variations in the volumes of the CDW and the AASW. Effects on the variation in properties of the AABW in the Amundsen Sea were analyzed in the horizontal direction based on the volume transport and heat transport at the three boundaries of the Amundsen Sea.

From 1993 to 2017, the thickness and volume of the AABW in the Amundsen Sea showed a decreasing trend, with rates of 5 m/a and 3.45×10^{12} m^3/a, respectively. The contraction of the AABW was accompanied by warming at a rate of approximately 0.002°C/a. This warming is equivalent to a heat flux of 0.27 W/m^2, and it produces a local SLR of 0.35 mm/a. The salinity increased during the study period, but the neutral density decreased by 0.000 3 kg/(m^3·a). Increasing temperature was likely the major factor driving the neutral density changes in the Amundsen Sea. In the vertical direction, the contraction of the AABW was compensated by the volume expansion of the CDW. Over the same period, the horizontal loss of the AABW volume was 4.07×10^{14} m^3 and the heat transport in the horizontal direction resulted in a 0.03°C increase in the temperature of the AABW.

The contraction of the AABW in the Amundsen Sea is due to a gradual decrease in the volume transport of the AABW along the pathway from the Ross Sea and compensation by the CDW. Part of the warming of the AABW in the Amundsen Sea is due to the decreasing and warming cold water inflow from the Ross Sea. These two variations in AABW in the Amundsen Sea can be traced back to the Ross Sea, where the variations are more dramatic. A reduction in the rate of AABW formation and changes in the properties of the AABW may be important causes of the variations.

Acknowledgements

Thanks to the anonymous reviewers for valuable comments that helped us improve this paper significantly.

References

Azaneu M, Kerr R, Mata M M, et al. 2013. Trends in the deep Southern Ocean (1958–2010): Implications for Antarctic Bottom Water properties and volume export. Journal of Geophysical Research: Oceans, 118(9): 4213–4227, doi: 10.1002/jgrc.20303

Carter L, McCave I N, Williams M J M. 2008. Circulation and water masses of the Southern Ocean: a review. Developments in Earth and Environmental Sciences, 8: 85–114, doi: 10.1016/S1571-9197(08)00004-9

Foster T D, Carmack E C. 1976. Frontal zone mixing and Antarctic Bottom Water formation in the southern Weddell Sea. Deep Sea Research and Oceanographic Abstracts, 23(4): 301–317, doi: 10.1016/0011-7471(76)90872-X

Ganachaud A, Wunsch C. 2000. Improved estimates of global ocean circulation, heat transport and mixing from hydrographic data. Nature, 408(6811): 453–457, doi: 10.1038/35044048

Jackson L C, Dubois C, Forget G, et al. 2019. The mean state and variability of the North Atlantic circulation: a perspective from ocean reanalyses. Journal of Geophysical Research: Oceans, 124(12): 9141–9170, doi: 10.1029/2019JC015210

Jacobs S S. 2004. Bottom water production and its links with the thermohaline circulation. Antarctic Science, 16(4): 427–437, doi: 10.1017/S095410200400224X

Jacobs S S, Fairbanks R G, Horibe Y. 1985. Origin and evolution of water masses near the Antarctic continental margin: Evidence from $H_2{}^{18}O/H_2{}^{16}O$ ratios in seawater. In: Jacobs S S, ed. Oceanology of the Antarctic Continental Shelf. Washington, DC: American Geophysical Union, 59–85, doi: 10.1029/AR043p0059

Jacobs S S, Giulivi C F. 2010. Large multidecadal salinity trends near the Pacific–Antarctic continental margin. Journal of Climate, 23(17): 4508–4524, doi: 10.1175/2010JCLI3284.1

Jacobs S S, Giulivi C F, Mele P A. 2002. Freshening of the Ross Sea during the late 20th century. Science, 297(5580): 386–389, doi: 10.1126/science.1069574

Johnson G C. 2008. Quantifying Antarctic bottom water and North Atlantic deep water volumes. Journal of Geophysical Research: Oceans, 113(C5): C05027, doi: 10.1029/2007JC004477

Johnson G C, Doney S C. 2006. Recent western South Atlantic bottom water warming. Geophysical Research Letters, 33(14): L14614, doi: 10.1029/2006GL026769

Johnson G C, McTaggart K E, Wanninkhof R. 2014. Antarctic Bottom Water temperature changes in the western South Atlantic from 1989 to 2014. Journal of Geophysical Research: Oceans, 119(12): 8567–8577, doi: 10.1002/2014JC010367

Johnson G C, Purkey S G, Bullister J L. 2008a. Warming and freshening in the abyssal southeastern Indian Ocean. Journal of Climate, 21(20): 5351–5363, doi: 10.1175/2008JCLI2384.1

Johnson G C, Purkey S G, Toole J M. 2008b. Reduced Antarctic meridional overturning circulation reaches the North Atlantic Ocean. Geophysical Research Letters, 35(22): L22601, doi: 10.1029/2008GL035619

Kawano T, Fukasawa M, Kouketsu S, et al. 2006. Bottom water warming along the pathway of lower circumpolar deep water in the Pacific Ocean. Geophysical Research Letters, 33(23): L23613, doi: 10.1029/2006GL027933

Koshlyakov M N, Tarakanov R Y. 2003. Antarctic bottom water in the Pacific sector of the Southern Ocean. Oceanology, 43(1): 1–15

Lumpkin R, Speer K. 2007. Global ocean meridional overturning. Journal of Physical Oceanography, 37(10): 2550–2562, doi: 10.1175/JPO3130.1

Mantyla A W, Reid J L. 1983. Abyssal characteristics of the World Ocean waters. Deep-Sea Research Part A. Oceanographic Research Papers, 30(8): 805–833, doi: 10.1016/0198-0149(83)90002-X

Masuda S, Awaji T, Sugiura N, et al. 2010. Simulated rapid warming of abyssal North Pacific waters. Science, 329(5989): 319–322, doi: 10.1126/science.1188703

Meredith M P. 2013. Oceanography: replenishing the abyss. Nature Geoscience, 6(3): 166–167, doi: 10.1038/ngeo1743

Meredith M P, Ducklow H W, Schofield O, et al. 2016. The interdisciplinary marine system of the Amundsen Sea, Southern Ocean: recent advances and the need for sustained observations. Deep-Sea Research Part II: Topical Studies in Oceanography, 123: 1–6, doi: 10.1016/j.dsr2.2015.12.002

Meredith M P, Gordon A L, Garabato A C N, et al. 2011. Synchronous intensification and warming of Antarctic Bottom Water outflow from the Weddell Gyre. Geophysical Research Letters, 38(3): L03603, doi: 10.1029/2010GL046265

Nardelli B B. 2020. A multi-year time series of observation-based 3D horizontal and vertical quasi-geostrophic global ocean currents. Earth System Science Data, 12(3): 1711–1723, doi: 10.5194/essd-12-1711-2020

Ohshima K I, Fukamachi Y, Williams G D, et al. 2013. Antarctic Bottom Water production by intense sea-ice formation in the Cape Darnley polynya. Nature Geoscience, 6(3): 235–240, doi: 10.1038/ngeo1738

Orsi A H, Johnson G C, Bullister J L. 1999. Circulation, mixing, and production of Antarctic Bottom Water. Progress in Oceanography, 43(1): 55–109, doi: 10.1016/S0079-6611(99)00004-X

Orsi A H, Smethie Jr W M, Bullister J L. 2002. On the total input of Antarctic waters to the deep ocean: a preliminary estimate from chlorofluorocarbon measurements. Journal of Geophysical Research: Oceans, 107(C8): 3122, doi: 10.1029/2001JC000976

Orsi A H, Wiederwohl C L. 2009. A recount of Ross Sea waters. Deep-Sea Research Part II: Topical Studies in Oceanography, 56(13–14): 778–795, doi: 10.1016/j.dsr2.2008.10.033

Ozaki H, Obata H, Naganobu M, et al. 2009. Long-term bottom water warming in the north Ross Sea. Journal of Oceanography, 65(2): 235–244, doi: 10.1007/s10872-009-0022-z

Patara L, Böning C W. 2014. Abyssal ocean warming around Antarctica strengthens the Atlantic overturning circulation. Geophysical Research Letters, 41(11): 3972–3978, doi: 10.1002/2014GL059923

Purkey S G, Johnson G C. 2010. Warming of global abyssal and deep Southern Ocean waters between the 1990s and 2000s: contributions to global heat and sea level rise budgets. Journal of Climate, 23(23): 6336–6351, doi: 10.1175/2010JCLI3682.1

Purkey S G, Johnson G C. 2012. Global contraction of Antarctic bottom water between the 1980s and 2000s. Journal of Climate, 25(17): 5830–5844, doi: 10.1175/JCLI-D-11-00612.1

Purkey S G, Johnson G C, Talley L D, et al. 2019. Unabated bottom water warming and freshening in the South Pacific Ocean. Journal of Geophysical Research: Oceans, 124(3): 1778–1794, doi: 10.1029/2018JC014775

Purkey S G, Smethie Jr W M, Gebbie G, et al. 2018. A synoptic view of the ventilation and circulation of Antarctic Bottom Water from chlorofluorocarbons and natural tracers. Annual Review of Marine Science, 10(1): 503–527, doi: 10.1146/annurev-marine-121916-063414

Reid J L. 1997. On the total geostrophic circulation of the Pacific Ocean: flow patterns, tracers, and transports. Progress in Oceanography, 39(4): 263–352, doi: 10.1016/S0079-6611(97)00012-8

Rintoul S R. 2018. The global influence of localized dynamics in the Southern Ocean. Nature, 558(7709): 209–218, doi: 10.1038/s41586-018-0182-3

Schmittner A, Chiang J C H, Hemming S R. 2007. Introduction: the ocean's meridional overturning circulation. In: Schmittner A, Chiang J C H, Hemming S R, eds. Ocean Circulation: Mechanisms and Impacts—Past and Future Changes of Meridional Overturning. Washington, DC: American Geophysical Union, 1–4, doi: 10.1029/173GM02

Shimada K, Aoki S, Ohshima K I, et al. 2012. Influence of Ross Sea Bottom Water changes on the warming and freshening of the Antarctic Bottom Water in the Australian-Antarctic Basin. Ocean Science, 8(4): 419–432, doi: 10.5194/os-8-419-2012

Uenzelmann-Neben G, Gohl K. 2012. Amundsen Sea sediment drifts: archives of modifications in oceanographic and climatic conditions. Marine Geology, 299–302: 51–62, doi: 10.1016/j.margeo.2011.12.007

van Wijk E M, Rintoul S R. 2014. Freshening drives contraction of Antarctic Bottom Water in the Australian Antarctic Basin. Geophysical Research Letters, 41(5): 1657–1664, doi: 10.1002/2013GL058921

Whitworth III T, Orsi A H, Kim S J, et al. 1985. Water masses and mixing near the Antarctic Slope Front. In: Jacobs S S, Weiss R F, eds. Ocean, Ice, and Atmosphere: Interactions at the Antarctic Continental Margin. Washington, DC: American Geophysical Union, 1–27, doi: 10.1029/AR075p0001

Zanowski H, Hallberg R, Sarmiento J L. 2015. Abyssal ocean warming and salinification after Weddell polynyas in the GFDL CM2G coupled climate model. Journal of Physical Oceanography, 45(11): 2755–2772, doi: 10.1175/JPO-D-15-0109.1